EFDA–JET–PR(10)67

M. Goniche, J. Mailloux, I. Coffey, A. Ekedahl, L. Delpech, P. Jacquet, J. Hillairet, K. Kirov, M.-L. Mayoral, D. Milanesio, R. Maggiora, J. Ongena, G. Sergienko and JET EFDA Contributors

Operational Issues at High LH Power Density in JET: Waveguide Conditioning and Arc Detection

Operational Issues at High LH Power Density in JET: Waveguide Conditioning and Arc Detection

M. Goniche[1], J. Mailloux[2], I. Coffey[2], A. Ekedahl[1], L. Delpech[1], P. Jacquet[2], J. Hillairet[1], K. Kirov[2], M.-L. Mayoral[2], D. Milanesio[3], R. Maggiora[3], J. Ongena[4], G. Sergienko[5] and JET EFDA Contributors*

JET-EFDA, Culham Science Centre, OX14 3DB, Abingdon, UK

[1]CEA, IRFM, F-13108 Saint Paul-lez-Durance, France
[2]EURATOM-CCFE Fusion Association, Culham Science Centre, OX14 3DB, Abingdon, OXON, UK
[3]Politecnico di Torino, Dipartimento di Elettronica, Torino, Italy
[4] Association EURATOM-Belgian State, Plasmaphysics Lab, Koninklijke Militaire School - Ecole Royale Militaire, TEC partner Brussels, Belgium
[5]Institute for Plasma Physics, Association EURATOM-IPP, D-52425 Jülich, Germany
** See annex of F. Romanelli et al, "Overview of JET Results", (23rd IAEA Fusion Energy Conference, Daejon, Republic of Korea (2010)).*

Preprint of Paper to be submitted for publication in
Plasma Physics and Controlled Fusion

ABSTRACT.
The power handling capability of the JET Lower Hybrid Current Drive(LHCD) system isexamined using the long-term database. The limitations, in particular in H-mode plasmas, are discussed and performances compared to other LHCD experiments using multijunctions as power dividers. Although the power density of 25MW/m^2 has been exceeded in L-mode and almost obtained in ELMy Hmode (on 1/6th of the antenna), it is concluded that the RF conditioning performed on JET does not allow to exceed an electric field of ~5.5kV/cm which is generally not sufficient in the rather weak coupling conditions of the JET H-mode. Modelling of an arc occurring in a waveguide indicates that rather small variations of the reflected wave (amplitude and phase) may occur rendering arc detection based on RF measurements difficult in some cases. The JET bolometry diagnostic with four chords viewing the antenna front is found to be an efficient tool to detect an arc. In L-mode plasmas, a very good correlation between the amplitude of the bolometry signals and the iron spectroscopic lines is found. In H-mode the arc detection is clearly more difficult with enhanced radiation during the ELM but is still possible when the bolometry signals are properly processed.

1. INTRODUCTION

Lower Hybrid (LH) range of frequency (1-8GHz) antennas are made from an array of narrow waveguides stacked in the poloidal and toroidal direction. The Radio Frequency (RF) power which can be coupled to the plasma is generally limited by the power transmission capability of these narrow waveguides facing the plasma. When this limit is exceeded, a breakdown in the very weakly ionized gas occurs inside the waveguides. This breakdown requires a fast interruption of the LH power to avoid, or at least limit, the erosion of the metallic plates of the waveguides and the resulting impurity release into the plasma.

This power limit is generally quoted in terms of power density (in units of MW/m^2) although the physical parameter controlling this limit is the amplitude of the high frequency electric field in the narrow waveguides (in units of V/m). When the forward and reflected field can be measured, there is a simple relation between these two quantities. When the antenna is composed of RF power dividers in the poloidal (3dB hybrid junction) and toroidal (the multi-junction) directions it is not straightforward to deduce the amplitude of the electromagnetic field in the narrow waveguides from RF measurements via directional couplers performed at the antenna input. In particular, in the E-plane multijunction, the wave undertakes back and forth travels before being reflected towards the generator allowing the power reflection coefficient to be of the order of R^n (where n is the number of passages of the forward wave) if the power reflection at the antenna-plasma interface is R. This great advantage for the generator operation is at the expense of the electric field amplitude which is strongly enhanced in the narrow waveguides of the multijunction by a factor $(1+R)^{n-1}$ with respect to the field in a conventional antenna. In fact, one needs a numerical code to compute this electric field which depends on the coupling of the antenna to the plasma and the details of the antenna structure.

LH antennas are in consequence designed to minimize the electric field with the best use of the available space in the port. In particular, for multijunction-type antenna, although different phasings of the waveguides are possible, the $\pi/2$ phasing minimizes the number of travels of the wave ($n = 2$) and therefore the electric field. Other considerations constrain the geometry: the required parallel refractive index of the launched wave ($N_{||}$) determines the width of the waveguides (b) along the magnetic field, the height (a) is such that the fundamental TE01 can only propagate ($a < \lambda_0$), the thickness of the septa must be sufficient for mechanical stiffness.

On JET, like on other tokamaks equipped with an LH system, the electric field limit is clearly seen and in particular when the plasma-antenna coupling weakens, for example in H-mode, breakdowns are detected generally by an increase of the reflection coefficient. However, the multijunction decouples, to some extent, the electric field at the input where the measurement is performed and the electric field at the output, near the plasma where the breakdown occurs and the Reflection Coefficient (RC) measured at the antenna input may not exceed the preset threshold for interrupting the power. Other methods can be used for diagnosing breakdowns, based on the light emitted either in the visible wavelength range (H_α/D_α lines), infra-red wavelength range (3-10mm) or very short wavelength (0.2-200nm, bolometry). All these techniques are efficient if the breakdown occurs very close to the plasma-antenna interface which is likely to be the most frequent case for the reason that the evanescent modes excited at this interface enhance the electric field at this precise location. Moreover, the electron density in the waveguides decays from the value required for wave coupling ($\sim 10^{17}$ m^{-3}) at the interface to ~0 on a finite length and this tenuous plasma is favourable for electron avalanche conducting to breakdown. However, breakdowns occurring deeper in the waveguides are not excluded and in this case detection can rely only on RF measurements or on light emission detected near the window assuming that the discharge propagates upstream which is the commonly accepted view.

In this paper, we describe the LH power handling capability on JET (section 2), then we discuss the theoretical limit, namely the multipactor effect and the control parameters (section 3). In section 4, a survey of breakdown or arc events from the 2000-2009 database with emphasis on the increase of the radiation from the launcher ('radiation event') is presented. The resulting impurity release is discussed. In the conclusion, we present some potential improvements of the protection system based on the bolometry diagnostic.

2. LH POWER LIMIT ON JET

The JET LHCD antenna detailed description can be found elsewhere [1,2,3]. The 48 waveguides, at the input of the antenna, are powered by 24 klystrons. For every input waveguide, the power is divided in order to feed 8 narrow waveguides (this unit is called module). This 8-fold division occurs in three steps along the wave propagation: first a division in the poloidal direction via a hybrid junction, second one in the toroidal direction via a primary bi-junction and finally a further division in the toroidal direction via a secondary bijunction. These two last power splitters

constitute the multijunction [4]. This arrangement leads to low power reflection towards the RF source and also simplifies the RF hardware. At the front face, the antenna is consequently an array of 12 rows of 32 waveguides facing the plasma (Figure 1), with 2 passive waveguides on each side to smooth the electric field at the edge and reduce ponderomotive effects. The dimension of one waveguide is $a \times b = 72 \times 9 mm^2$. For RF source protection, a circulator diverts most of the reflected power towards a dummy load. This component allows quite high reflection coefficients from the antenna and the generator is switched off when the reflected power exceeds 22kW (resp. 32kW) for a forward power of 200kW (resp.400kW). However, an arc at the grill mouth will not necessarily result in a significant increase in reflected power (see section 4). For that reason, the 'Imbalance Protection System', developed to protect against arcs at the grill mouth, monitors the difference between, and the ratio of, the reflected power from the upper and lower modules powered by the same klystron (RPU and RPL respectively). The trip levels are adapted for each klystron, and are not necessarily symmetrical, to take into account the fact that RPU and RPL can be significantly different even during normal operation on some klystron units. For example, the power of klystron A3 is interrupted for typically 100ms (adjustable) if RPU-RPL > 16 kW AND RPU/RPL > 3, or if RPL-RPU > 35kW AND RPL/RPU > 3. The asymmetry in the trip levels is because RPL is much greater than RPU on A3 during normal operation. However, in some cases, the arcs at the grill mouth are not identified fast enough by that system, and melting of the waveguides can take place before the arcs are interrupted, as described later in this paper. This is due, at least in part, to the fact that the trip levels must be high enough to avoid an excessive number of trips during ELMy plasmas (during an ELM, RPU and RPL in a same unit can vary differently, presumably because of temporary poloidal asymmetries in the SOL density)

On L-mode plasmas, 7.3MW (Pulse No: 33618) has been coupled for 0.2s during a 5s pulse with many trips and 6.2MW (Pulse No: 34419) for 2s in more steady conditions [5]. These two coupled powers correspond to a power density of 29 and $25 MW/m^2$ respectively. More in detail, the power handling capability is not found homogeneous across the whole radiating surface of the launcher. Depending on the plasma equilibrium, the poloidal shape of the antenna does not always fit the flux surfaces and for most pulses the distance of the antenna to the plasma is larger in the bottom part of the antenna and consequently the coupling there weakens. Scanning the JET database (1993-2009), it is found that the power coupled in the bottom rows of waveguides, normalized to the power coupled to the upper rows, decreases when this mismatch increases (figure 2). When gas is injected from a pipe with poloidally distributed holes located near the antenna, the power coupled by the lower rows increases with respect to the upper rows, suggesting more efficient fuelling in front of the lower part of the antenna. At the same time, the coupling imbalance, evaluated from the ratio of the mean RC of the bottom rows to that of the lower rows increases. As a result, the higher power output per row is not obtained simultaneously on all rows. However, on each third of the antenna (each third corresponds to four rows of 32 waveguides fed by 8 klystrons) powers of 2.4-2.5MW ($\sim 29.5 MW/m^2$) averaged over 1s have been achieved on several shots.

On ELMy H-mode plasmas, the power handling capability is reduced. This is partly the result of the steep density profile in the scrape-off layer combined with the large mismatch between flux surfaces and the antenna in case of high triangularity plasmas. The density in front of the launcher is then close to the cut-off density (nco) and a power reflection coefficient exceeding 10% is measured between the ELMs. The situation can be greatly improved by injecting gas from a pipe magnetically connected to the antenna [6, 13]. In such conditions, up to 3.2MW (13MW/m^2) could be coupled with an antenna-plasma distance as large as 15cm [7]. However, on 1/6th of the surface (upper left part) the average power density reached (23MW/m^2) for 2s which is just 20% less of what has been achieved in L-mode, averaged on the whole antenna (figure 3). During the ELM burst, the edge density measured by a reciprocating Langmuir probe magnetically connected to the LH antenna can have a ten-fold increase but this increase of density is generally beneficial for coupling high LH power. Modelling with the ALOHA code [10,11] shows that i) the maximum electric field decreases monotonically when the density increases to values close to the perfectly coupled (RC = 0) situation (figure 4-a) ii) the RC increases for n/nco>4 but is kept quite low (RC < 5%) for the entire antenna if we consider that the density does not exceed 3×10^{18} m^{-3} and when the TM evanescent modes are included with the fundamental propagating TE01 mode (figure 4-b). From this modelling we thus do not expect a reduced handling power capability due to either an increase of the electric field or to an increase of the RC which could require the power to be interrupted for protection of the klystron. This renders in effect the multijunction 'ELM resilient': indeed, a detailed analysis of the RF signals does not show power trips during the ELM bursts. Assuming an electric field limit of 5kV/cm, deduced from LH operation on Tore Supra equipped with a very similar launcher, the density has to be, between ELMs, ~3 times the cut-off density for coupling a power density of 25MW/m^2, a condition which could be scarcely fulfilled on JET even with local gas injection.

During the ELM burst, edge density can have a ten-fold increase and the flux of fast electrons accelerated in the near field is expected to increase accordingly [8]. However we do not observe an increase of impurity related to the ELM activity and computation shows that this transient heat flux does not significantly contribute to the thermal response of the plasma facing components magnetically connected to the antenna [7]. Operation at higher electric field is possible but needs more dedicated time, and probably intensive conditioning of the antenna prior to the experiments. It should be noted that the number of LH pulses in ELMy plasma is much smaller than in L-mode plasmas, furthermore, little time has been dedicated to try to push the LH power under these conditions.

The high neutral pressure within the waveguides has been sometimes evoked as possible reason for reducing the power handling capability. In fact the neutral pressure is expected to favour arcing when the mean free path of electrons in a gas of pressure P is lower than the typical dimension of the waveguide which occurs when P exceeds ~1Pa. On JET the tank in which the 3m long antenna is installed is evacuated by a cryo-pump having a pumping speed of ~80m^3/s [9] but the effective pumping speed of the waveguides, via holes drilled in the walls of the modules, does not exceed

~0.1m^3/s, except for the front end of the antenna which is pumped by the plasma with a speed, estimated from the pressure decay when the plasma current is ramped-up, of the order of 10m^3/s. The base pressure, measured in the tank before launching LH power, is below 5×10^{-5} Pa in most cases. Taking into account the conductance between the waveguides and the tank and also the pumping provided by the plasma, the pressure in the multijunction is estimated to be 3-10 times higher. During the LH pulse, this pressure increases but this pressure exceeds 1.5×10^{-3} Pa (up to 3.5×10^{-3} Pa) for only 14 pulses (out of 4156 for the 2001-2009 database) from which 8 are very low magnetic field (1T) pulses not representative of standard operation (figure 5). We can therefore assess that the pressure within the waveguides does not increase beyond 10^{-2} Pa and that the pressure is likely not to be a limiting parameter. The pressure histogram also does not show any correlation with the LH coupled power (quoted here from the highest power averaged on a gliding time window of 1s): whatever the power level, the most frequent pressure increase is of the order of 1×10^{-4} Pa. However gas coverage of the waveguide walls increases breakdown hazard, as discussed in next section, and pressure for a given pumping speed is an indication of the These performances can be compared to other multijunction antennas installed on Petula, JT-60, JT-60U and Tore Supra.

On Petula, which used a multijunction operated at 3.7GHz with 3 secondary waveguides, a power density of 96MW/m^2 was achieved when all the available power was injected in one module of 2 rows of 3 waveguides [19]. This was achieved for a maximum duration available from the klystron of 30ms. However the very high outgassing rate on this short time scale (at least one order of magnitude higher than the highest rate measured on JET) indicates that such power density could not probably be achieved on long pulses. JT60 and JT60-U developed the same kind of multijunction and later a large multijunction with 12 secondary waveguides operated at 2GHz [10, 11]. For these two types of antenna, a power density of 27 and 25MW/m^2 was achieved respectively for ~1s in L-mode discharges. On Tore Supra, the two LHCD launchers (1989-1998 and 1990-2008) use a 4 secondary waveguide multijunction with dimensions very close to that of the JET antenna. A power density of 39MW/m^2 (with a RC of 2%) was achieved for 1s with one of these launchers [12], but almost twenty years of experience showed that after reasonable conditioning a power level of 25MW/m^2 could be quite easily obtained and the Tore Supra database shows more than 300 pulses with such a power density for a duration exceeding 3s. A slightly lower level (23.5MW/m^2) was also sustained for 75s. More recently a new type of multijunction, the passive-active multijunction, has been tested up to 75MW/m^2 for 0.9s at 8GHz on FTU [13] and at larger scale up to 25MW/m^2 for 77s at 3.7GHz on Tore Supra [14]. For this last experiment, work is still is progress and the actual limit still to be explored. It should be noted that for this type of antenna, the passive waveguides inserted between the waveguides fed by the multijunction also radiate RF power, thanks to the strong coupling between waveguides via the plasma, and the surface of these waveguides could also been considered for the calculation of the power density. In that case, the power density is reduced to 37MW/m^2 for the 8GHz experiment and 14MW/m^2 for the 3.7GHz experiment.

In order to have a comprehensive understanding of the power limit for systems operated at

different frequencies with different antenna designs, the underlying mechanism of breakdowns in waveguides is examined in the following section.

3. OVERVIEW OF BREAKDOWN PHYSICS IN RF WAVEGUIDES

Whereas RF electric field exceeding 10kV/cm is currently achieved in ICRF antennas operated in the 20-80MHz range, breakdowns in the narrow waveguides of LHRF antennas (1-8 GHz) occur generally at lower field. The reason is that the limiting process differs: in the ICRF case, power transmission capability is limited by field emission and in the LHRF case by the multipactor effect. Both phenomena cause ionization and electron avalanche by surface effects. The multipactor effect which can affect RF sources (klystrons) as well as evacuated waveguides has been studied in detail [15, 16, Ryopoulos95, 17, 18]. When the transit time of an electron from a waveguide wall to the opposite wall τ is equal to an even number of half the period of the wave T (τ /T= n/^{2}, n is called the order of the multipactor), the electrons are continuously submitted to an accelerating electric field and can gain a kinetic energy of several hundreds eV. With such energy, the secondary electron yield g of the surface can exceed one which is a necessary condition for electron avalanche. In the case of an antenna installed on a tokamak, a static magnetic field perpendicular to the electric field has to be added in the motion equation. In that case, there are in fact four criteria for multipactor to occur and the details can be found in [Ryopoulos95]. Solving the equation of motion of the electron, the driving force can be expressed with the dimensionless parameter $\varepsilon = eE_{RF}/m_e\omega^2 d$ where ERF is the amplitude of the electric field, $\omega/2\pi$ the frequency of the wave, d the distance between the walls of the waveguide, e and m_e the electric charge and mass of the electron, respectively. Finally the lower limit of electric field E_{min} for first order multipactoring (multipactor occurs for a range of electric field) can be expressed as $E_{min} = f(B, \gamma)\ \omega^2 dd$ where $f(B, \gamma)$ is a function of the magnetic field and secondary electron yield. In fact full multipactoring calculations show that E_{min} does not scale with $\omega^2 d$ but simply with ωas the order of the multipactoring increases with increasing value of ωd [18]. The electric field limit will be dependent on the magnetic equilibrium (B) and on the surface state (γ). For this second point, γ can significantly increase when going from a clean metallic surface to an oxidised surface or a surface with adsorbed gas (H_{20}, CO, CO_2). This coefficient is unknown for the LH launcher and probably evolves with the conditioning of the machine. In particular, carbonization is expected to be favourable as carbon coated surface (especially rough coatings with the extreme case of soot which has a yield much lower than one for all energies of primary electrons) has shown the lowest yield. Adsorbed gas and oxides can be removed by glow discharge which has to be done at rather high pressure (>10Pa) in order to be stable and uniform in narrow waveguides [19]. High temperature baking ($T \geq 300°C$ for several hours) is also efficient [20, 21] and electric field strengths as high as 6.6kV/cm have been reached for long pulses (>100s) on a 3.7GHz antenna multijunction module tested on a matched load without external magnetic field. However even with such high temperature baking which is not always easy to carry out for an antenna when installed in the tokamak, the power handling capability is improved gradually

by accumulating RF pulses either on vacuum between plasma pulses (which means without the confinement magnetic field) or on plasma. This method has proven to be efficient on all tokamaks. The beneficial effect of this technique, although time-consuming, is two-fold: i) power transmission is accompanied by RF losses which heat up the waveguides walls (in particular on vacuum when the power reflection is high) ii) breakdowns in the waveguides and formation of a Townsend discharge or a glow discharge can occur. Both effects are beneficial for removing the oxides and adsorbed gases and in this respect low outgassing flux during power transmission is a reliable signature of good conditioning. However, if the discharge transits to the arc regime characterized by an increase of the electron current by several orders of magnitude, the waveguides surface can be severely damaged when not detected on a sufficiently short time scale.

On JET, the waveguides are not actively heated. After a shutdown with atmospheric pressure venting, JET is generally baked at 320°C for more than 20 days. The plates ending and surrounding the part of the LH launcher outside the torus are brought to the same temperature as JET (in some restarts, it is maintained above that temperature, by ~50°C). The temperature of the waveguides is measured with thermocouples placed near the H-plane junction in each multijunction, and is ~200°C typically in JET and the LH surrounding plate is at 320°C (~140°C if JET and the surrounding plates are at 200°C). The pressure measured in the LHCD tank (which depends also on the pressure in the torus) goes down (typically to $\sim 1\times10^{-4}$ Pa) at the end of this high temperature baking. As soon as the pressure is lower than 5×10^{-3} Pa, conditioning on vacuum is performed to increase further the waveguide temperature. Two techniques have been used on JET, either ~3-second pulses with up to ~150kW/klystron or 10ms pulses with a duty cycle of 1/10 and up to ~200kW/klystron. In both cases, the klystrons are pulsing simultaneously and consequently the reflected power results also from the waveguide cross-coupling which is difficult to predict in vacuum. The power reflection coefficients vary widely from one module to another: from values below 10% to values exceeding 70%. We can estimate the maximum electric field strength at the antenna opening from the coupling code ALOHA which was run with an edge density varying between 1 and 40×10^{17} m^{-3}. The power reflection coefficient of the 8 modules aligned on a row varies from very low values (<1%) to RC~80%. The scaling of the maximum electric field Emax with RC is found to be close to that predicted from a simple analytical formula obtained when the wave is assumed to travel twice back and forth in the multijunction before reflection to the antenna input (figure 6). This calculation also assumes that the phase shift of the wave reflected at the plasma –antenna interface is the same for the 4 waveguides of the multijunction. Assuming the same relation between the measured RC and E_{max} on vacuum, we conclude that vacuum conditioning at the level of 200kW (resp. 150kW) is effective if the RC is at least 30% (resp. 70%) in order to provide a field of 5.5kV/cm required for operation on plasma at high power (6.2MW, 25MW/m^2) with RC ≤ 5%.

4. ARC DETECTION AND IMPURITY RELEASE DURING JET PULSES

For RF systems, arcs are usually detected from RF measurements and the power reflection

coefficient, measured at the input of the antenna, generally increases when an arc occurs in a narrow waveguide. However, this is not always the case for a multijunction antenna and the RC may be weakly affected or decreases. This point was investigated with the help of TOPLHA code [24] by modelling an arc as a short-circuit of width $\Delta a = 4$mm (the waveguide height is $a = 72$mm), which is a rough approximation in the arc regime (the current density is then very high) and provides at least an estimate of the maximum effect on RC one can expect. The RC is mostly sensitive to this change of plasma-antenna coupling when the plasma density is low. When an arc occurs (assumed to be in waveguide 2 of module 5 in this example) , the RC increases by 4-5% for density in the $2\text{-}5\times10^{17}$ m^{-3} range whereas the phase shift is only ~10° (figure 7). At higher density, the increase of RC is smaller (1-2%) but the phase shift is much larger ~40°.

In simulations of arcs, the result differs from the case where the two concerned waveguides are fed by the two secondary bi-junctions (waveguide 2 and 3) to the case where the waveguides are fed by the same secondary bi-junction (waveguide 1 and 2). In the first case, compensation occurs because of the symmetry of the configuration, and the RC increase is smaller than that in the one arc case or can even decrease (for ne=2×1017m-3, case shown in figure 7). In the second case, the increase of RC is about twice that for an arc case. It should be noted, that the RC and the phase of the reflected wave in the adjacent modules is weakly affected: the RC does not change by more than ±1% (1.5% in the case of two arcs) and the phase shift is at the most 10° (20° in the case of two arcs). When the arc does not propagate up to the module input, we can conclude from this modelling that a protection system based on detection of changes in the RC (amplitude or phase) measured at the input of a multijunction antenna will not detect the arc in most cases. This detection can be even more difficult with RC variations caused by non stationary coupling conditions resulting from high frequency density fluctuations (which can very large in the scrapeoff layer) or ELMs. In fact this modeling indicates that the electric field in waveguides adjacent to one where an arc occurs increases (or decreases) by up to 30%, and consequently the breakdown may propagate from waveguide to waveguide. This is a frequent situation based on imaging (visible or infra-red light): generally arcing is observed across all waveguides in a row.

On JET, the bolometry diagnostic was found to be efficient to detect arcs occurring at the antenna front, and especially during arcs that are not stopped early by the protection system based on the reflected power measurements described in 2). The bolometry camera is located in an upper port of the torus at the same toroidal position with the LHCD launcher and, since 2005, 4 chords (ch.1, 2, 3 and 4) of this diagnostic view the rows of waveguides facing the plasma (figure 8-a). In fact for ch.1 (resp. ch.4), only a small fraction of the beam is viewing the top (resp. bottom) of the antenna. Moreover, the angle of the line-of-sight decreases from ch.4 to ch.1 and the sensitivity of the signal to the radiation emitted from the launcher decreases. Figure 8-b shows the signals (in W/m^2) for these 4 channels when they have been weighted under the assumption that the light emission from the launcher before pulsing is uniform all across its surface. The present protection system is based on the signal of ch.2 offset from ch.4 which is assumed to be the background emission.

When the antenna is launching power smoothly (i.e. with no arcs near the antenna front), these bolometry signals increase quite moderately, typically a factor of 2 with 3MW. For the pulse of figure 8-b, the increase of radiation is larger from the top with respect to the bottom of the antenna For this pulse, the bottom channel (Ch.4) reference has a very weak increase with respect of the reference channel (ch.5, not shown). This increase is partly the result of increase of density caused by enhanced ionization provided by a small fraction of the LH waves which is dissipated near the antenna. The top/bottom asymmetry is attributed to the shorter distance between the antenna and the plasma at the top. The strong increase of ch.1 and ch.2 at the start of the power injection followed by a slow decay is consistent with the slow increase of the RC (from ~3 to ~4%) for the upper and middle rows (edge density decreases). At t=15.7s, power generators feeding half of the upper and middle rows are interrupted and emission from the top and middle (ch.1 and ch.2) decrease by 35% and 15 % whereas emission from the bottom (ch.3 and ch.4) does not change, confirming the spatial resolution of this diagnostic and the sensitivity of these measurements to the local density of electrons, ions and possibly impurities (at the onset of the LH power, the transient increase of radiation for ch.1 and ch.2 is correlated to a transient increase of the CIII line by a factor 3-4). From a large data base of plasma pulses heated by LHCD only and covering the 2005-2009 JET campaigns, it is found that the time–averaged amplitudes of these four channels (with ground radiation from ch.5 subtracted) increases linearly with LHCD power (0.5-5.3MW). Comparing the four channels, it is found that the average radiation is the highest for ch1 (resp. ch.2) for 54% (resp. 41%) of the pulses whereas the radiation from the bottom of the antenna is maximum in few cases. However a large number of the pulses (~30-40%) have a significantly larger radiation than the linear scaling with LHCD power, up to a factor 10. It can be speculated that this is the result of discharges occurring at the extremity of one or several waveguides and depending on the nature of the discharge (glow discharge, beneficial or arc discharge, deleterious) and the spatial extension (number of waveguides), the radiation enhancement can widely vary. When an arc occurs with metal release, the increase of radiation is partly due to the electron density increase due to the strong outgassing of over-heated surfaces but also from metal atoms sputtered/ evaporated from the waveguide surface. These atoms are ionized more deeply in the plasma and depending on the line-of-sight, the spatial resolution in the poloidal direction could be affected.

In H-mode, with large additional power provided by Neutral Beam Injection (NBI) and ion cyclotron resonance heating (ICRH), the radiation is higher and strongly modulated by the ELMs and the evolution of the radiation due to the LHCD power is not easily seen, although, on a statistical basis, we found on average more radiation at high LHCD power ($P_{LHCD} > 2MW$). This wide range of radiation values from the launcher is much more evident when one focuses on the instant values instead of values averaged over the LHCD pulse duration. Figure 9 shows two H-mode plasmas with evidence of arcs at the grill mouth unstopped by the protection system based on reflected powers. The radiation is modulated by the ELMs bursts. The increase of the radiation provoked by arcs can nevertheless be detected. In the first pulse the radiation increases in two steps (at t = 5.9s

and t = 8s). Large impurity release (>1×10^6) occurs at the second step when the radiation from the antenna exceeds ~1.5×10^5W/m^2 and is attributed to an arc event at the launcher aperture. In the second case, with also two steps (at t = 20.9s and 21.7s), large impurity release also occurs when the radiation exceeds about the same level. It should be noted that in the first case, the radiation is the highest for the channel viewing the upper part of the antenna and in the second case for the channel viewing the lower part. This difference is related to the position of the antenna with respect of the plasma. For the first case, the plasma is farther by 2cm from the upper part whereas the distance is unchanged for the bottom part. RF measurements indicate consistently strong variations of the RCs when the radiation increases. In the first case, the RC of a middle row module increases from 1 to 10% and in the second case, the RC of some lower modules increase from 1% to 5%, at the same time as the first increase of radiation. More generally, a fairly good correlation is found between the maximum radiation and the iron release. For the pulses in L-mode with LHCD only (figure 10-a), when the maximum of radiation does not exceed 1.5×10^5 W/m^2, the intensity of the FeXXIII line is low (3×10^5). In H-mode with high NBI power (P_{NBI} >10MW), the maximum of radiation is typically 10-fold larger with ELMs and low metal contamination of the plasma (Figure 10-b). High iron influx ($I_{FeXXIII} \sim 1\times10^7$) can be obtained when a strong arc occurs ($I_{Bolo} \sim 1\times10^6$W/m^2) but conversely when the LH power is switched off sufficiently early, impurity influx can be kept low. This is the case for the 2 points at the far right of figure 10-b with high radiation (~1×10^7W/m^2) and relatively low FeXXIII line intensity ($I_{FeXXIII} < 3\times10^6$).

These graphs also show that the arcs are mainly located in the upper waveguides (ch.1 and 2) in H-mode with large additional power (>10MW) as in L-mode with LHCD only. When the impurity influx is too high, the plasma discharge can disrupt, especially in L-mode plasmas. This occurs mainly in the commissioning phase of the LHCD antenna and the 27 discharges of the 2008-2009 campaign that disrupted following arcs were analyzed. These discharges, all in L-mode, almost half of them with low NBI power (<2MW), are characterized by an increase of the radiation before the LHCD system is switched off either at the preset time or when an arc is detected by the protection system. In these discharges, some klystron powers are often interrupted momentarily by the protection system based on reflected power but clearly the imbalance protection system does not detect all arcs for all modules. On figure 11 is shown the delay between the time when one of the 4 bolometry signals exceed a threshold (1×10^5W/m^2) and the time the LHCD system is switched off. This time varies between ~20ms and 1s. For very short delay, lower than 50ms (4 discharges), the disruption could probably not be avoided, but for the others we expect that the metal release could have been sufficiently reduced for preventing from radiation collapse. It should be noted that the threshold level (normalized to a line-integrated density $n_l = 5\times10^{19}$ m^{-2}) is rather accurately determined to be 1×10^5W/m^2 since in many cases the maximum radiation flux does not exceed 1-2$\times10^6$W/m^2 range which is still one order of magnitude higher than that of the arc-free discharges.

For H-mode discharges, the optimal threshold to prevent significant impurity release (Fe>2×10^6) is found to be around 1.5×10^6W/m^2 after 250Hz low-pass filtering and proper weighting of the

bolometry signals. Conversely, figure 9b shows that in many cases, the maximum of radiation can exceed 1×10^6 W/m^2 without low impurity production. This is the case when the protection system detects an arc and switches off the LHCD power sufficiently early. It is also the case when a giant ELM is triggered. In that case, the estimated threshold of is exceeded by about a factor 3. A short interruption of the power, of the order of 100ms, when the threshold is exceeded should not affect too much the average coupled power as these events are not very frequent.

CONCLUSIONS

Although power density close to 25MW/m^2 has been achieved on JET in L-mode but also in Hmode (on 1/6th of the antenna for this latter case) when the coupling is sufficiently good, i.e. when the edge density exceeds at least 2 or 3 times the cut-off density, the power is limited in most high performance plasma scenarios by breakdowns in the waveguides. The electromagnetic analysis of the antenna coupled to the plasma shows that electric field limit is in the 5.0-5.5kV/cm range. Clearly the limited baking capability of the antenna (~200°C) and the conditioning on vacuum (limited to 250kW) do not allow going beyond this limit. Without improvement of the coupling which in principle could be obtained either by a better alignment of the magnetic flux surfaces with the antenna front shape or by an improved optimization of the near antenna gas injection, the only improvement could be obtained from the conditioning procedure which could be done at higher power (~400kW with short pulses) and more regularly during the experimental campaigns, in particular on modules with low reflection coefficient on vacuum.

In the antenna commissioning phase when the LH power is increased from pulse to pulse, breakdowns cannot be avoided. Breakdowns can also occur because the coupling conditions evolve from one pulse to another and the electric field may increase with unchanged LH power. A breakdown can be very detrimental if it turns into an arc. The RF protection system based on reflected power measurements at the antenna input is found not sufficient for arc detection. When the number of secondary waveguides of the multijunction increases, required for very large antennas, the system is expected to be even more insensitive to the change of impedance due to an arc located near the opening of a secondary waveguide. On JET, the vertical bolometry camera viewing the antenna is an efficient tool to detect arcs with fast response (~5ms) and some spatial resolution (~30cm) allowing not switching off the whole generator when an arc is detected. For Lmode discharges, we found that a threshold on the radiation flux from the launcher can be used as part of the protection system aiming at reducing the metal contamination and the disruption occurrence. More precisely, a threshold of 1×10^5W/m^2 is likely to be the optimum, in particular for preventing the plasma from disruptions. In ELMy plasmas, the analysis of the few shots for which a large impurity influx was measured indicate that, provided the signal is adequately low-pass filtered and the threshold optimized between 1 and 2×10^5W/m^2, arc detection can be efficient but remains more difficult. Further analysis on a larger database would be necessary to precise the optimal strategy depending probably on the recycling conditions, ELM frequency and amplitude. The geometrical configuration of the diagnostic

is not optimal as the line-of-sight viewing the top of the antenna is very tangential to the magnetic surfaces and antenna front face. On ITER, using the spatial resolution of this diagnostic with more favourable lines-of-sight, the reduction of power could be of the order of 10% only when an arc is detected from enhanced radiation from the launcher [25]. In the next JET experimental campaign, a visible camera and an infrared camera viewing the antenna will be available. This will allow to confirm more precisely the location of the arcs and to correlate the measurements of these new diagnostics with the signals of the bolometry

ACKNOWLEDGEMENT

This work, supported by the European Communities under the contract of Association between EURATOM and CEA, was carried out within the framework of the European Fusion Development Agreement. The views and opinions expressed herein do not necessarily reflect those of the European Commission. The authors are grateful to Prof. Kishek and Dr Vicente for fruitful discussions on multipactoring.

[1]. Litaudon, X., Moreau, D., Nuclear Fusion **30** (1990) 471.
[2]. Lenholm M et al 1995 Proc. 16th IEEE/NPSS Symp. Fusion Engineering (Urbana-Champaign, Illinois, 1995) vol 1, p 754
[3]. Schild Ph. et al 1997 Proc. 17th IEEE/NPSS Symp. Fusion Engineering (San Diego, CA, 1997) vol 1, p 421
[4]. Nguyen T.K. and Moreau D. in Proc. of the 12th Symp. on Fus. Technol. 1982, vol.2, pp 1383-1386
[5]. Ekedahl A. et al., Plasma Physics and Controlled Fusion, **5** (1998) 315-334
[6]. Ekedahl A. et al., Plasma Physics and Controlled Fusion **51** (2009) 044001 (17pp)
[7]. Goniche M. et al., Plasma Physics and Controlled Fusion **51** (2009) 044002 (18pp)
[8]. Jacquet P. et al, submitted to Nuclear Fusion
[9]. Dobbing J.A. , Ekedahl A., Finburg P., Fischer B, Gormezano C, Lennholm M, Romero J, Schild P. and Söldner F.X., Power Handling in the JET Lower Hybrid Launcher, JET report JET–R(97)06
[10]. Ikeda Y. et al., Plasma Devices and Operations, Vol.1, 155-181 (1991)
[11]. Seki M.et al., Fusion Science Technology, **42** (2002) 452-466
[12]. Goniche M. et al. Europhysics Topical Conference of RF heating and current drive, Bruxelles, European Physical Society, Vol.**16**E, 69-72 (1992)
[13]. Pericoli Ridolfini V., Nuclear Fusion **45** (2005) 1386–1395
[14]. Ekedahl A. et al., Nuclear Fusion **50** (2010) 112002.
[15]. Farnsworth P.T, J.Franklin Inst. **218**, 411 (1934)
[16]. Hatch A.J. and Williams H.B., Physical Review, **112**, 681-685 (1958)
[17]. Kishek R.A. et al., Physics of Plasmas, **5** (1998) 2120-2126

[18]. Vicente C. et al., IEEE, 2006
[19]. Rey G. et al., 15th Symp.on Fusion Technol., North-Holland, 514-517 (1988)
[20]. Goniche M. et al., Journal of Vacuum Science Technology, A **23**(1), 55-65 (2005)
[21]. Kossyi I A. et al., Journal of Physics D: Applied Physics **41** (2008) 065203 (8pp)
[22]. Hillairet J. et al., Nuclear Fusion **50** (2010) 125010 (17pp)
[23]. Preynas M. et al., Nuclear Fusion **51** 023001 doi: 10.1088/0029-5515/51/2/023001
[24]. Milanesio D., Lancelloti V., Meneghini O., Maggiora R., Vecchi G. and Bilato R. 2007 TOPLHA: an accurate and efficient numerical tool for analysis and design of lh antennas Proc. 17th Topical Conf. on Radio Frequency Power in Plasmas AIP Conf. Proc. (Clearwater, Florida,USA, May 2007) 933 301–4 http://scitation.aip.org/
[25]. Hoang G T et al 2009 Nuclear Fusion **49** 075001

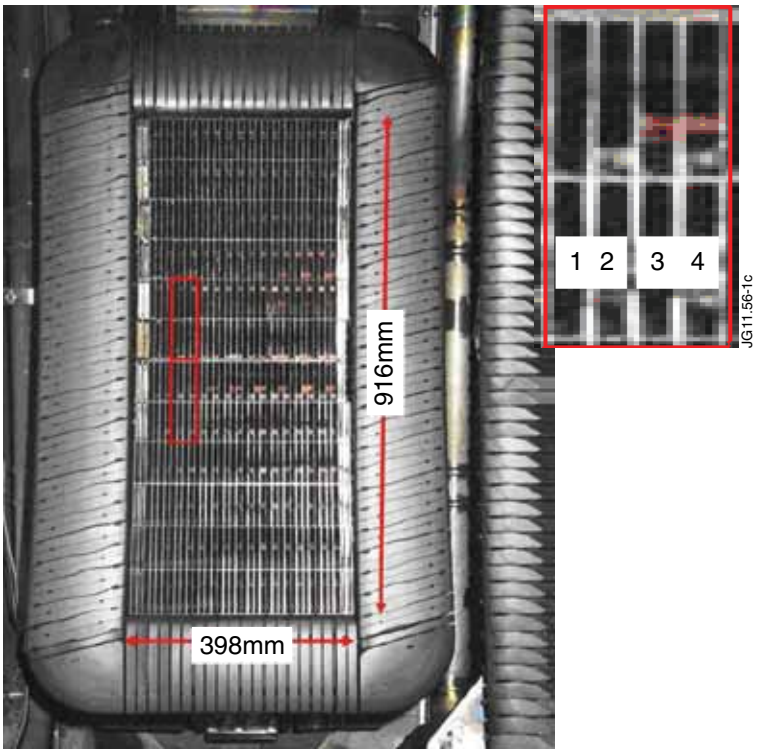

Figure 1: The JET LHCD antenna. Two modules fed by the same klystron are highlighted. Numbering of waveguides is given in the blow-up of a module.

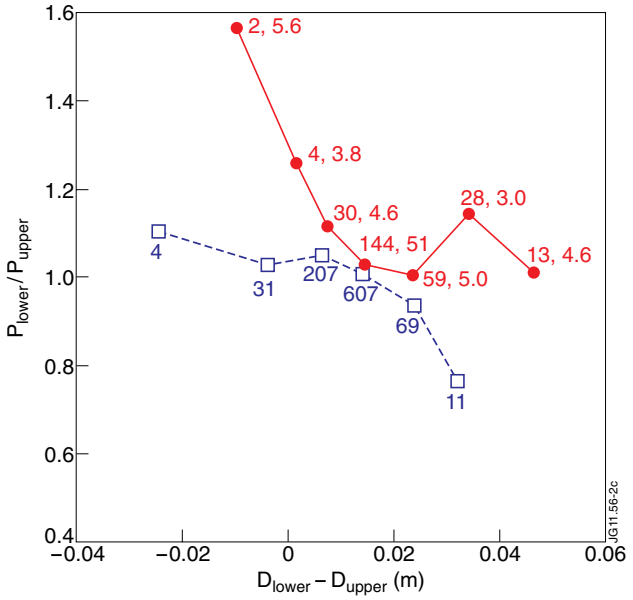

Figure 2: Power imbalance as a function of the mismatch between the shape of the antenna and the LCFS for pulses without (dotted line) and with (solid line) local gas injection. Number of pulses on which the data are averaged and average gas rate (in 10^{21} el./s) are shown.

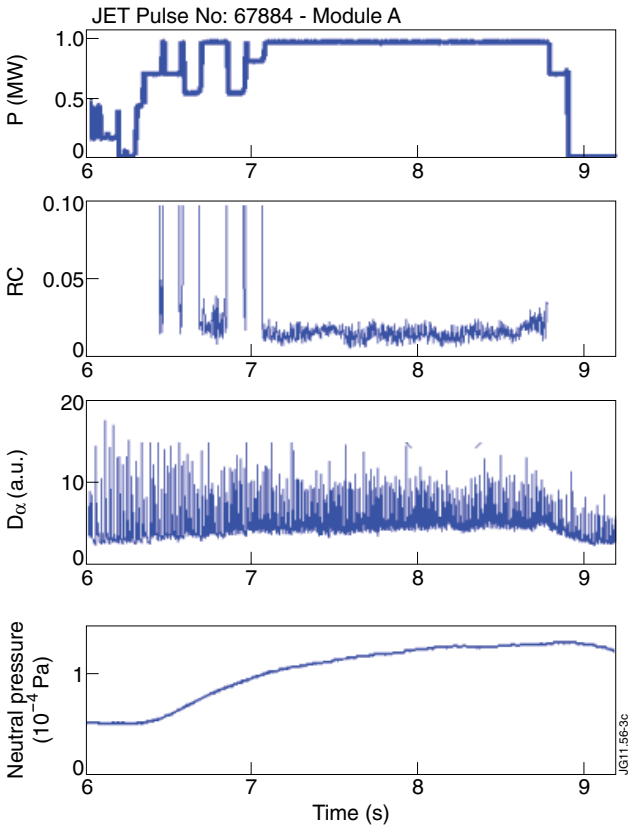

Figure 3: Forward power and RC for an H-mode pulse. The power density is 23MW/m^2 (1/6th of the antenna). Antenna-LCFS distance is 13cm.

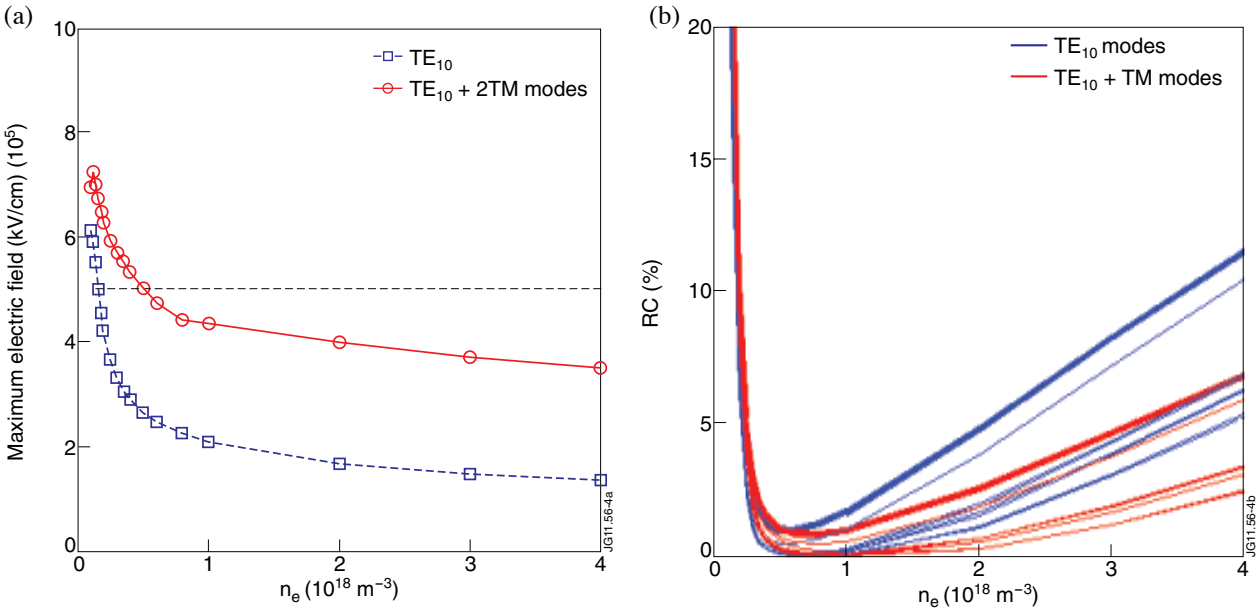

Figure 4: a) Maximum electric field for $P_{forward}$ = 6.2MW (25MW/m^2) at the antenna-plasma interface for module 1b) Reflection coefficients at the antenna input for the 8 modules (thick lines are module 1) as a function of electron density.

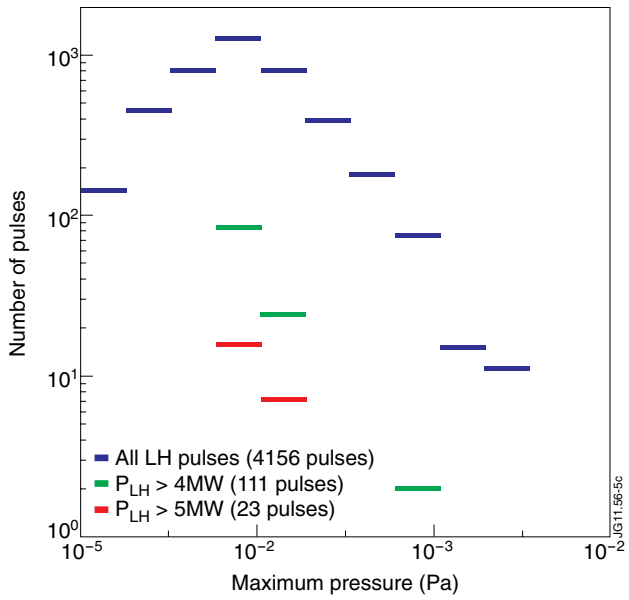

Figure 5: Histogram of maximum neutral pressure in the antenna tank. The quoted LH power is the highest power averaged on a sliding time window of 1s (JET 2001-2009 database).

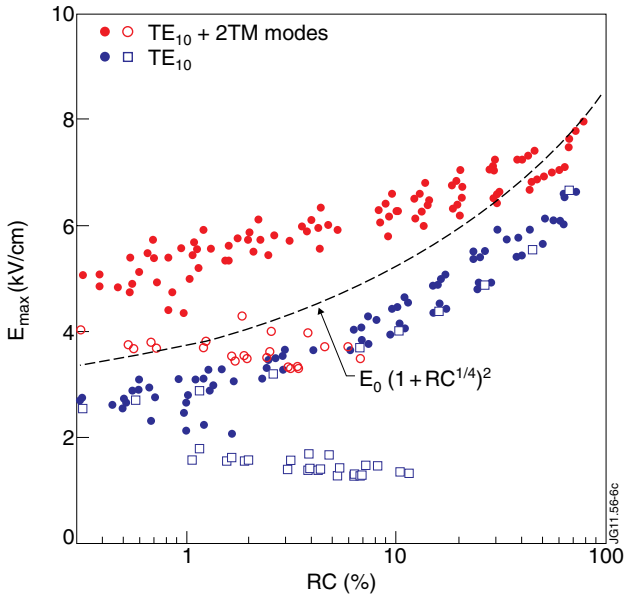

Figure 6: Maximum electric field at the antenna opening as a function of the reflection coefficient measured at the input of the antenna modules. The electron density is varied between $1\times10^{17}m^{-3}$ (n/nco~0.6) and $10\times10^{17}m^{-3}$ (closed symbols), between $20\times10^{17}m^{-3}$ and $40\times10^{17}m^{-3}$ (open symbols). The values of the 8 modules constituting a row of the JET antenna are plotted. The input power is 130kW per module (260kW per klystron), corresponding to a power density in the multijunction of $25MW/m^2$. ALOHA modelling.

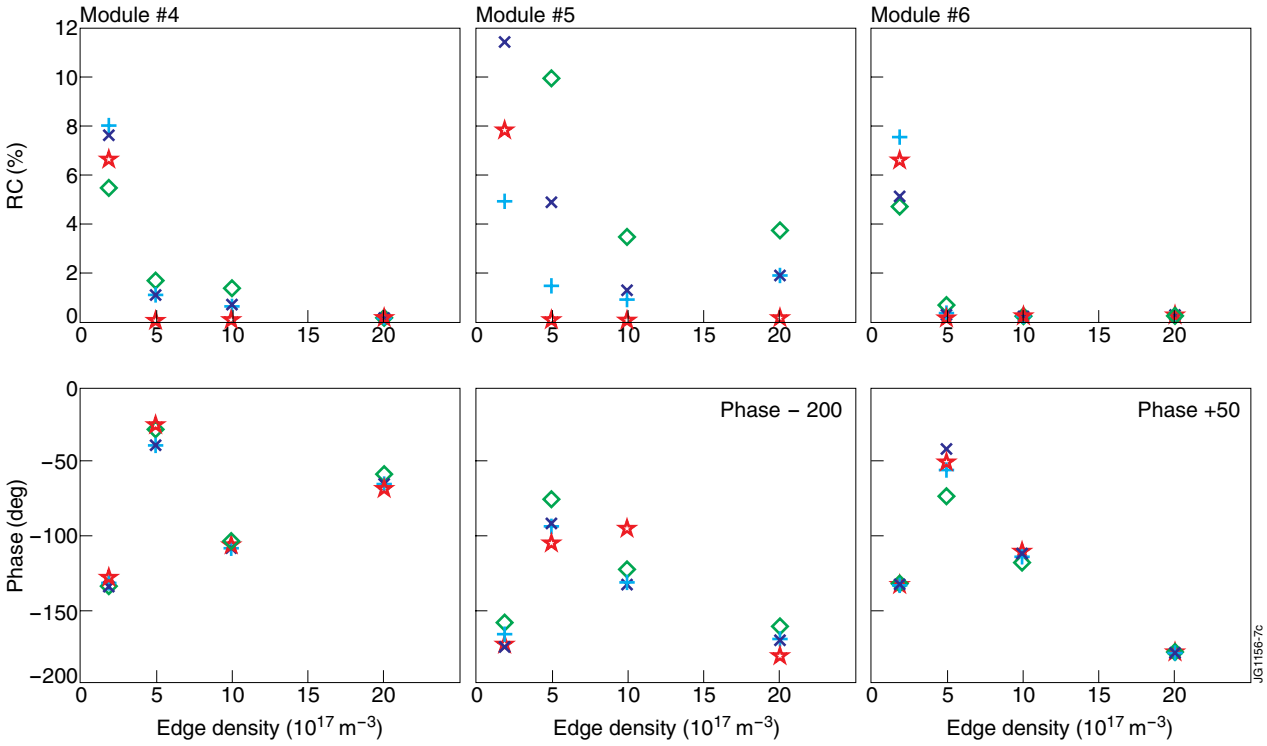

Figure 7: Effect of a short-circuit in waveguide 2 (× blue symbol), 2 and 3 (+ blue symbol), 1 and 2 (◊ green symbol) of module 5 on the RC (top) and phase of the reflected wave (bottom). Reference with no arc is also shown (red symbol). TOPLHA modelling. The symmetry axis of the antenna lies between module 4 and 5.

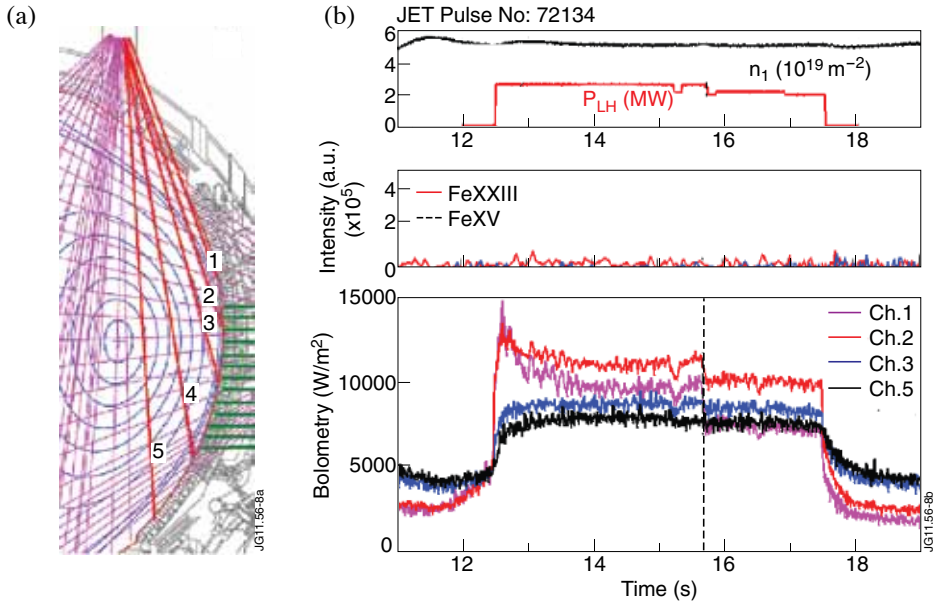

Figure 8: a) Poloidal cross section of JET showing the 12 rows of the LHCD launcher, the bolometry lines-of-sight and the magnetic flux surfaces. b) Time traces of LHCD power, lineintegrated plasma density (top), impurity spectroscopic lines (FeXV and FeXXIII) intensity (middle), bolometry channels viewing the LHCD launcher (bottom).

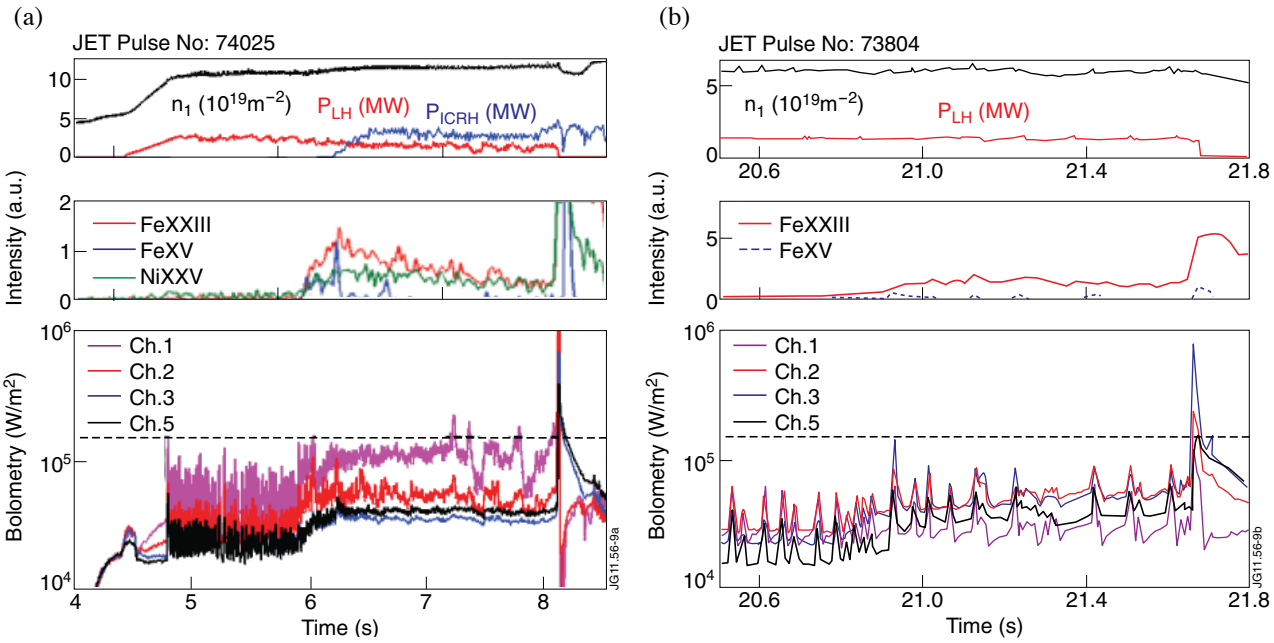

Figure 9: Time traces of LHCD power, line-integrated plasma density (top), impurity spectroscopic lines (FeXV and FeXXIII) intensity (middle), bolometry channels viewing the LHCD launcher (bottom) for H-mode plasmas a) Pulse No: 74025 b) Pulse No: 73804. Bolometry signals have been lowpass filtered (250Hz).

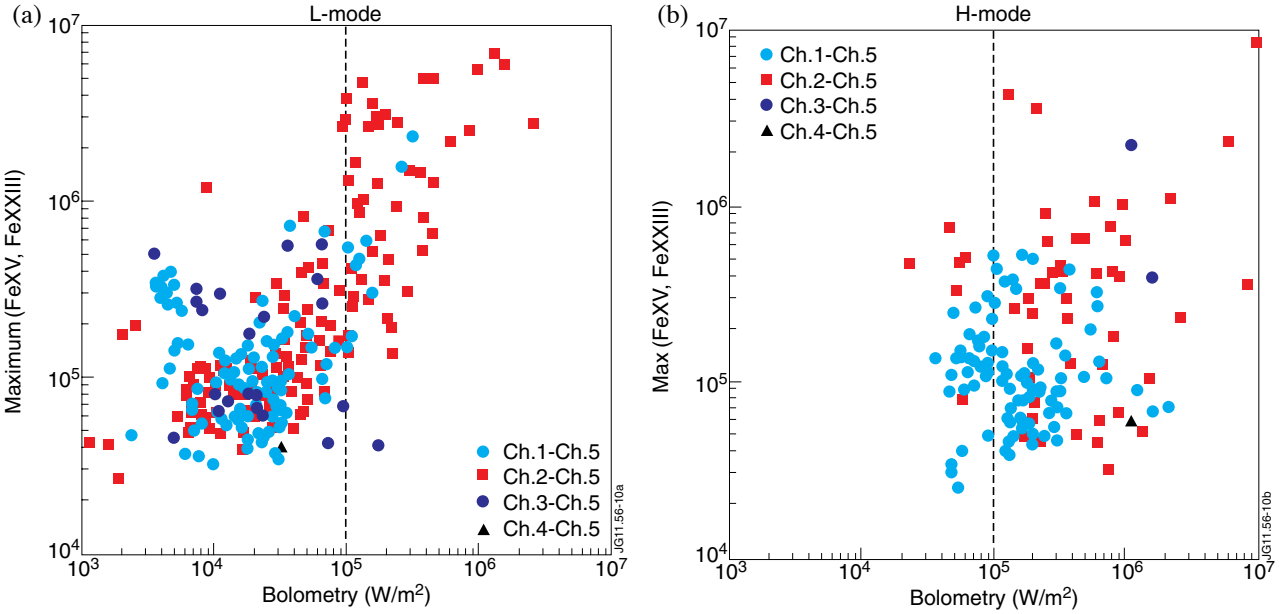

Figure 10: Maximum intensity of the FeXV or FeXXIII lines as a function of the highest signal of the bolometry channel. a) L-mode pulses, b) H-Mode pulses. All signals are normalized to the line-integrated density. Background signal (from ch.5) is subtracted to bolometry signals.

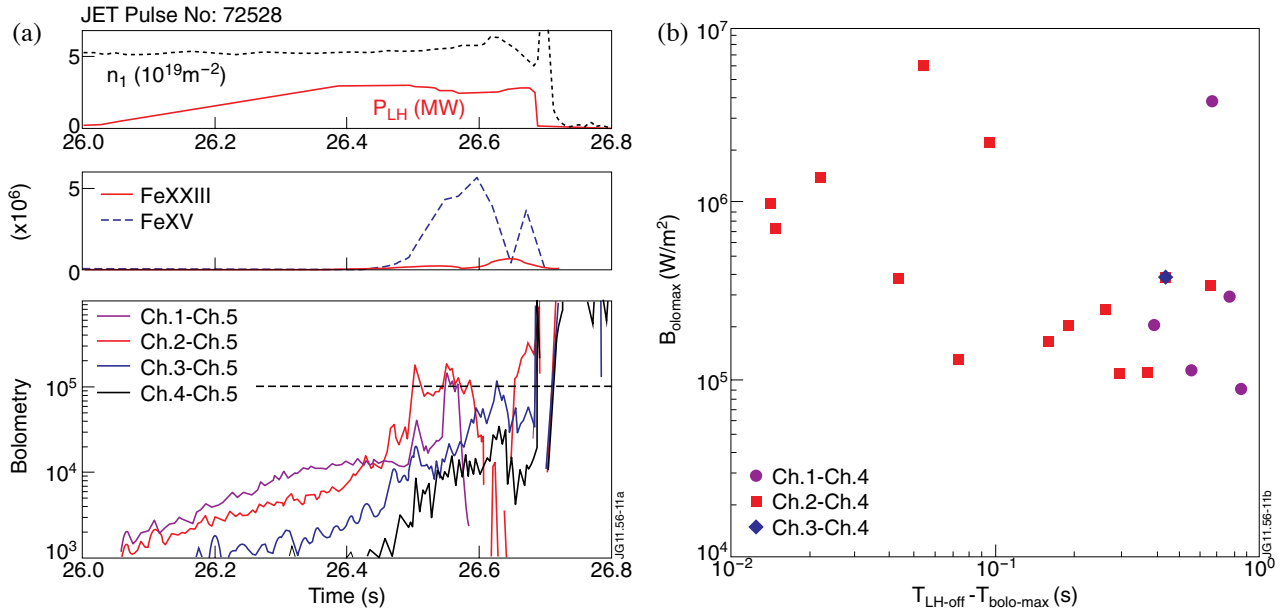

Figure 11: a) Time traces of LHCD power, line-integrated plasma density (top), impurity spectroscopic lines (FeXV and FeXXIII) intensity (middle), bolometry channels viewing the LHCD launcher (bottom) for a L-mode plasma terminated by a disruption, b) Maximum of the bolometry signals versus delay between the time when the bolometry signals exceed the threshold and the time the LHCD system is switched off.